

THERMAL DILEPTON RATES AND IN-MEDIUM HADRON PROPERTIES FROM LATTICE QCD

I. WETZORKE

*NIC/DESY Zeuthen,
Platanenallee 6,
D-15738 Zeuthen, Germany
E-mail: Ines.Wetzorke@desy.de*

Recent progress of lattice investigations in thermal physics is summarized in this contribution. Hadronic spectral functions can be reconstructed from correlation functions in Euclidean time based on the Maximum Entropy Method without a priori assumptions on the spectral shape. The thermal modifications of hadron properties are investigated in the scalar, pseudo-scalar, vector and axial-vector channels near and above the deconfinement transition temperature for charmonium systems as well as for light quarks. Moreover, the reconstructed vector meson spectral function allows to extract the thermal cross section for the production of dilepton pairs at vanishing momentum.

1. Introduction

Precise lattice QCD calculations of hadron masses and decay constants at zero temperature were performed in the recent years. A challenge is the investigation of modifications of hadronic properties at finite temperature, in particular the changes of the spectral shape. The spectral functions are directly relevant for experimental annihilation cross sections in relativistic heavy-ion collisions, e.g. the temperature dependence of the vector meson mass and width is related to changes of the thermal dilepton spectrum.

On the lattice the particle masses are usually obtained from the exponential decrease of the correlation function at zero momentum at large Euclidean times τ :

$$G(\tau) = \int d^3x \langle J_H(\vec{x}, \tau) J_H^\dagger(\vec{0}, 0) \rangle \sim e^{-m\tau}, \quad (1)$$

where the hadronic current $J_H(\tau, \vec{x}) = \bar{\psi}(\tau, \vec{x}) \Gamma \psi(\tau, \vec{x})$ is given in the scalar, pseudo-scalar, vector or axial-vector channel with $\Gamma \in [\mathbf{1}, \gamma_5, \gamma_\mu, \gamma_\mu \gamma_5]$. At finite temperature T the Euclidean time extent is restricted by $1/T$ ren-

dering a reliable determination of the particle masses increasingly difficult with rising temperature.

Another possibility to extract the masses and decay constants is provided by the hadronic spectral functions σ_H , which are related to the correlation functions in Euclidean time by

$$G(\tau, \vec{p}) = \int d^3x e^{i\vec{p}\vec{x}} \langle J_H(\tau, \vec{x}) J_H^\dagger(0, \vec{0}) \rangle = \int_0^\infty d\omega K(\tau, \omega) \sigma_H(\omega, \vec{p}, T), \quad (2)$$

where K is the integration kernel in the continuum

$$K^{cont}(\tau, \omega) = \frac{\cosh(\omega(\tau - 1/2T))}{\sinh(\omega/2T)}. \quad (3)$$

The reconstruction of a smooth spectral function given only a limited number of points of the correlator in Euclidean time can be classified as typical ill-posed problem. Previous analyses have been done under restricting assumptions on the spectral shape. The modern solution is provided by the Maximum Entropy Method (MEM), which has been applied successfully to many similar problems in physics¹. This approach has been first applied in lattice QCD by². It allows to obtain the most probable spectral function without a priori assumptions on the spectral shape by maximizing the prior probability in addition to usual least-square minimization.

2. Meson spectral functions at $T = 0$ and $T = \infty$

Before we proceed to hadronic spectral functions at finite temperature, where very little is known about the spectral shape so far, the behavior in the limiting cases $T = 0$ and $T = \infty$ should be investigated. At zero temperature δ -function like peaks are expected for the ground and excited states at low energies, while the meson spectral functions should be proportional to ω^2 at high energies. The precise quenched QCD data of the CP-PACS Collaboration has been used for a detailed MEM analysis of ground and excited state meson masses as well as decay constants³. They have investigated pseudo-scalar and vector meson correlators on very large lattices ($32^3 \times 56$ to $64^3 \times 112$) to at four different values of the lattice spacing a . The pseudo-scalar spectral function $\rho(\omega) = \sigma_{PS}/\omega^2$ in figure 1 shows several peaks for the ground and excited states. On smaller lattices only the ground state⁴ and one excited state² can be resolved by the reconstructed spectral function. In general the peaks are broader and reduced in height for smaller lattice sizes and lower statistics.

The ground state masses extracted from the spectral functions are the same as the ones obtained from exponential fits of the correlator, while the mass of the first excited state could be determined much more precisely than before. The broad state slightly below $\omega a = 2$, similarly observed in ^{4,2}, diverges in the continuum limit (fig. 1 right) and thus has been identified as unphysical lattice artifact (cut-off effect) of the heavy fermion doublers appearing in the Wilson type fermion formulations.

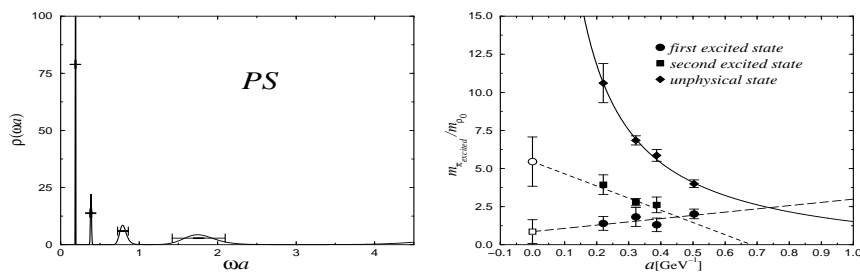


Figure 1. Pseudo-scalar spectral function at $T = 0$ (left) and continuum extrapolation (right) taken from ³, results for the vector meson are similar.

At finite temperature excited states and continuum-like contributions are expected to gain in influence on the spectral shape. The spectral functions at $T = \infty$ for free massless quarks are known from leading order perturbation theory, e.g. $\sigma_{PS}^{free} = 3/8\pi^{-2}\omega^2 \tanh(\omega/4T)$. It is mandatory to verify that MEM allows to reconstruct such a continuum-like shape correctly. It turned out ⁵ that this shape cannot be obtained using the continuum integration kernel of eq.(3) due to large contributions of heavy Wilson fermion doublers at high energies. The application of the finite lattice approximation of the continuum kernel

$$K^{lat}(\tau, \omega) = 2\omega/N_\tau \sum_{n=0}^{N_\tau-1} \frac{\exp(-i \omega_n \tau)}{4 \sin^2(\omega_n/2) + \omega^2} \quad (4)$$

absorbs the cut-off effects efficiently and allows an almost perfect reconstruction already for 8-16 points in Euclidean time. The MEM analysis reported in the following sections is therefore performed using this lattice adapted integration kernel.

In a very recent paper ⁶ the authors studied the cut-off effects in detail in the infinite temperature limit, where the spectral functions can be calculated analytically ⁷. They found considerable cut-off effects for the usual

Wilson fermion formulation, which are strongly suppressed and shifted to the very high energy regime using a truncated perfect fermion action.

3. Medium modifications for light mesons

The thermal changes of meson spectral functions in the light quark sector have been investigated in the range 0.4-3.0 times the chiral phase transition temperature. The simulations were performed in quenched QCD with a non-perturbatively improved fermion action on large isotropic lattices up to $64^3 \times 24$. Calculations below T_c were carried out at non-vanishing quark mass corresponding to a pion mass of about 500 MeV. Above the critical temperature the simulations could be performed directly at approximately zero quark mass, since massless Goldstone modes are no longer present.

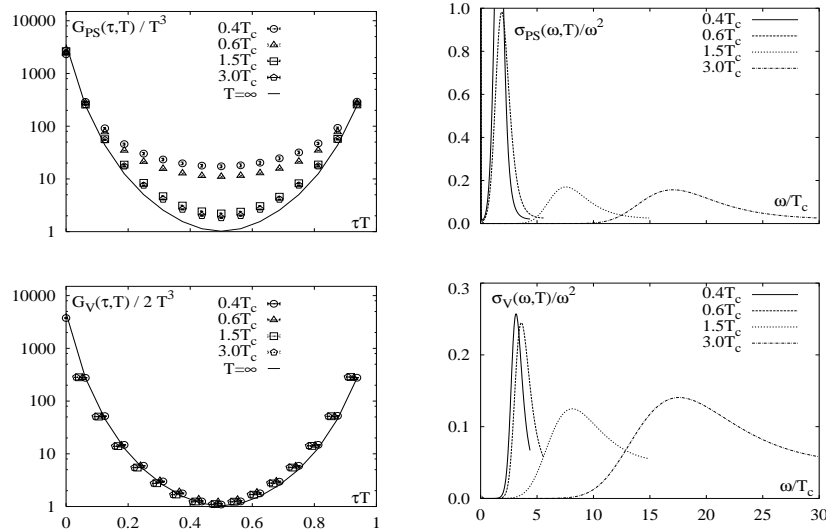


Figure 2. Light pseudo-scalar (top) and vector meson (bottom) correlation (left) and spectral functions (right) in the range 0.4 to 3.0 T_c taken from ⁸. Points of the vector meson correlators are slightly displaced for better visibility. Only the low energy part of the spectral functions is given, which is not affected by cut-off effects ⁹.

Figure 2 shows the modifications of the zero momentum correlation and reconstructed spectral functions in the investigated temperature range. While crossing the phase transition temperature the change of the pseudo-scalar correlator is clearly obvious. Above the critical temperature the

correlation function slowly approaches the free meson correlator indicated as solid line, while the vector meson correlator is near the free curve for all temperatures. The corresponding spectral functions show a pronounced ground state peak below T_c , which is transformed into a broad bump at higher energies above T_c . In fact, this remnant of the ground state peak scales with the temperature and thus its position remains almost the same when plotted in units of ω/T instead of ω/T_c .

Moreover, a degeneracy of the pseudo-scalar and scalar iso-vector correlation and spectral functions could be observed above the critical temperature indicating effective chiral $U_A(1)$ symmetry restoration.

A more quantitative picture of the deviations from the free quark behavior can be obtained by taking the ratio of the correlator with the corresponding free meson correlator for the same lattice size, which is illustrated in figure 3. In the pseudo-scalar channel one can still observe a considerable deviation from the propagation of a free $q\bar{q}$ pair even at a temperature as high as $3 T_c$ indicating a remnant of the strong interaction between the quarks above the chiral phase transition. The situation is different in the vector channel. The correlator ratio visualizes that the vector meson correlation function shows only a 10 % deviation from the free quark behavior. Furthermore, the value of $G_V(1/2T, T)/T^3$ is finite, which implies that the spectral function σ_V has to vanish in the limit $\omega \rightarrow 0$. The determination of the slope of the spectral function at $\omega = 0$ would be of major interest, since finite values for the transport coefficients of the QGP would require $\sigma \sim \omega$ in this limit ¹¹. Unfortunately, simulations on even larger lattices would be needed to increase the sensitivity of the reconstructed spectral functions in the very low energy region.

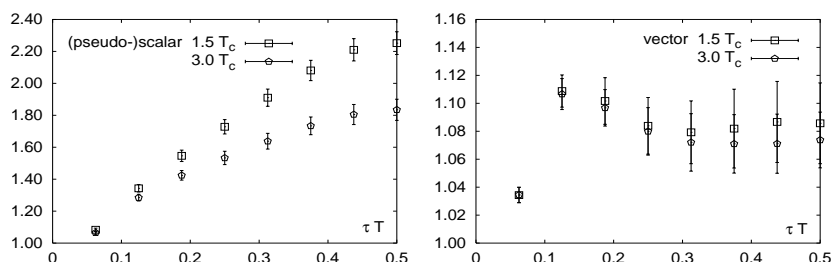


Figure 3. Correlator ratios $G(\tau T)/G_{free}(\tau T)$ for the pseudo-scalar (left) and vector meson (right) taken from ¹⁰.

4. Thermal dilepton rates

The thermal dilepton spectrum is accessible in heavy ion collisions and provides an important observable to study thermal properties of the medium at high temperature and density^{12,13}. The non-perturbative in-medium modifications of the $q\bar{q}$ interactions are expected to influence thermally induced changes of the dilepton spectrum at low energies¹⁴. The differential dilepton rate in two-flavor QCD is directly related to the spectral function in the vector channel

$$\frac{dN_{l\bar{l}}}{d^4x d^4p} \equiv \frac{dW}{d\omega d^3p} = \frac{5\alpha^2}{27\pi^2} \frac{1}{\omega^2 (e^{\omega/T} - 1)} \sigma_V(\omega, \vec{p}, T). \quad (5)$$

The left hand side of figure 4 gives a detailed error estimate on the vector meson spectral function which is used to calculate the dilepton rate. The dashed band illustrates solely the statistical error, while the vertical lines illustrate the uncertainty of the MEM reconstruction in the given ω/T ranges. Moreover, calculations with different lattice spacings and volumes have been performed to ensure that the spectral shape of σ_V is not influenced by cut-off or finite volume effects in the given energy regime⁹.

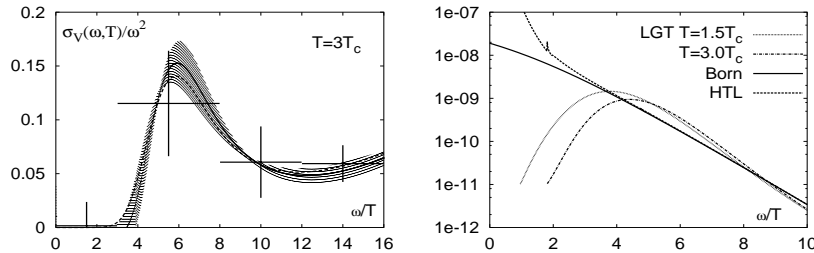


Figure 4. Vector meson spectral function (left) and thermal dilepton rate at $p = 0$ (right) taken from^{10,8}.

The thermal cross section for the production of dilepton pairs at vanishing momentum (right side of fig.4) is obtained by applying eq.(5) for the vector meson spectral function. The leading order perturbative result (Born rate) and a calculation in HTL-resummed perturbation theory^{15,16} are given for comparison. A small enhancement over the Born rate in the range 4-8 ω/T is visible for the lattice gauge theory (LGT) result at both temperatures, whereas the rate decreases rapidly at smaller energies. This

behavior is in clear contrast to the hard thermal loop calculations, which predict a divergent result in the infrared limit.

It is evident that perturbative as well as lattice calculations should investigate the low energy regime in more detail. An obvious step in this direction is to try to enhance the sensitivity of the statistical analysis of thermal correlation functions in the low energy region. A first attempt along this line has recently been tested in a calculation of the electrical conductivity and soft photon production rate of the QCD plasma ¹⁷.

5. Charmonia

For the heavy $c\bar{c}$ bound states the situation is different from the light quark sector. Potential model calculations predict a sequential dissolution, where higher excitations like $\chi_{c,0}$ [3P_0] and $\chi_{c,1}$ [3P_1] dissolve earlier, while the s-wave states J/ψ [3S_1] and η_c [1S_0] may survive after the deconfinement phase transition ¹⁸.

Three different lattice QCD groups have investigated charmonium spectral functions so far. The simulations have been performed on large isotropic ¹⁹ and anisotropic lattices ^{20,21} covering the temperature range 0.9 to 1.9 T_c . The thermal modifications of the charmonium spectral functions found by ¹⁹ are displayed in figure 5 for the pseudo-scalar (η_c and similar the vector meson J/ψ) and for the axial-vector channel ($\chi_{c,1}$ and similar for the scalar $\chi_{c,0}$) at 0.93 and 1.25 T_c . The left figure shows that the pronounced ground state peaks for the J/ψ and η_c survive even at 1.25 T_c , while a drastic change can be observed in the spectral functions of the orbitally excited states $\chi_{c,0}$ and $\chi_{c,1}$. The second broad bump at higher energies in both pictures is most likely a cut-off effect as discussed above.

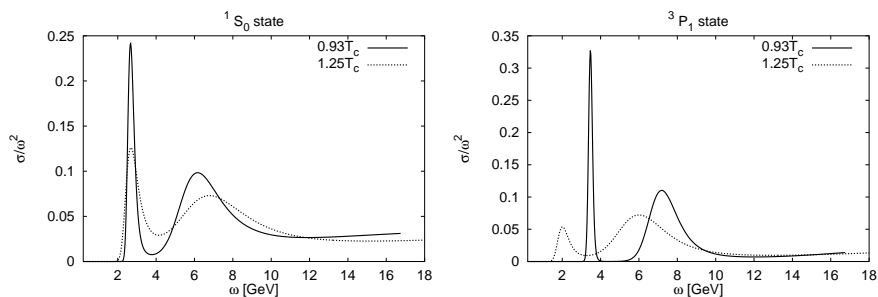


Figure 5. Thermal changes of charmonium spectral functions in the pseudo-scalar (left) and axial-vector channel (right) taken from ¹⁹.

The results on anisotropic lattices support this finding of sequential dissolution. The survival of sharp ground state peaks at $1.1 T_c$ has been reported for the pseudo-scalar (η_c) and vector channel (J/ψ)²⁰, while a near degeneracy of the spectral functions in all channels has been observed at $1.9 T_c$ indicating chiral symmetry restoration²¹. Combining the results of all groups one may conclude that the orbitally excited states dissolve in the vicinity of the deconfinement phase transition temperature, while the J/ψ and η_c persist as bound states up to $1.25 T_c$ and probably dissolve in the range $1.5 - 1.9 T_c$.

6. Conclusions & Outlook

The application of the Maximum Entropy Method for the reconstruction of spectral functions from correlation functions in Euclidean time without a priori assumptions on the spectral shape initiated the recent progress of lattice investigations in thermal physics. Already at zero temperature this approach leads to more precise predictions of the masses of excited states, but the most important point is that the study of hadronic spectral functions at finite temperature became feasible. New insight could be obtained in the in-medium modifications of hadronic properties in the vicinity and above the phase transition temperature.

Deviations from the free quark-antiquark propagation could be observed in the pseudo-scalar channel up to $3 T_c$, while the vector meson correlation and spectral function are much closer to the free quark behavior. Above the critical temperature an effective $U_A(1)$ symmetry restoration between the pseudo-scalar and scalar iso-vector states has been found. The thermal dilepton production rate could be calculated for the first time from lattice QCD data using the spectral function in the vector meson channel. Finally, the pattern of sequential dissolution of the heavy charmonium states is supported by the spectral analysis.

Further investigations will be certainly needed in the vicinity of the critical temperature and in the low energy region. All the lattice QCD calculations reported in this summary were performed in the quenched approximation, which neglects the influence of virtual quark loops. The extension to simulations with dynamical quarks will be the major challenge in the future.

Acknowledgments

Parts of the work summarized in this talk emanate from a very lively collaboration with F. Karsch, E. Laermann, S. Datta, P. Petreczky and S. Stickan. Furthermore, I want to thank the organizers of the Villefranche Workshop on Quantum Chromodynamics for the invitation.

References

1. For a review see: M. Jarrel and J.E. Gubernatis, Phys. Rep. 269, 133 (1996).
2. Y. Nakahara et al., Phys. Rev. D60, 091503 (1999);
M. Asakawa et al., Prog. Part. Nucl. Phys. 46, 459 (2001).
3. T. Yamazaki et al. (CP-PACS Coll.), Phys. Rev. D65, 014501 (2002).
4. I. Wetzorke and F. Karsch, in Proceedings of the International Workshop on Strong and Electroweak Matter 2000 (Edt. C.P. Korhals-Altes, World Scientific 2001), p.193, hep-lat/0008008.
5. I. Wetzorke et al., Nucl. Phys. Proc. Suppl. 106, 510 (2002).
6. F. Karsch et al., arXiv:hep-lat/0303017.
7. D.B. Carpenter and C.F. Baillie, Nucl. Phys. B260, 103 (1985).
8. F. Karsch et al., Nucl. Phys. A 715, 701 (2003).
9. S. Stickan, arXiv:hep-lat/0301009.
10. F. Karsch et al., Phys. Lett. B530, 147 (2002).
11. G. Aarts and J. M. Martinez Resco, JHEP 0204, 053 (2002).
12. J. Kapusta, Phys. Lett. 136B, 201 (1984).
13. L.D. McLerran and T. Toimela, Phys. Rev. D31 (1985) 545;
J. Alam et al., Annals Phys. 286, 159 (2001).
14. M.C. Abreu et al. (NA50), Phys. Lett. B450, 456 (1999).
15. E. Braaten et al., Phys. Rev. Lett. 64, 2242 (1990);
P. Aurenche et al., Phys. Rev. D58, 085003 (1998).
16. M.G. Mustafa et al., Phys. Rev. C61, 024902 (1999);
F. Karsch et al., Phys. Lett. B497, 249 (2001).
17. S. Gupta, arXiv:hep-lat/0301006.
18. F. Karsch and H. Satz, Z. Phys. C 51, 209 (1991).
19. S. Datta et al., arXiv:hep-lat/0208012.
20. T. Umeda et al., arXiv:hep-lat/0211003.
21. M. Asakawa et al., arXiv:hep-lat/0208059.